

Supporting information

Hierarchical Sheet-on-Sheet Heterojunction Array of $\beta\text{-Ni(OH)}_2/\text{Fe(OH)}_3$ Self-Supporting

Anode for Effective Overall Alkaline Water Splitting

Baoqiang Wu, Zhaoxi Yang, Xiaoping Dai,* Xueli Yin, Yonghao Gan, Fei Nie, Ziteng Ren,
Yihua Cao, Zhi Li, Xin Zhang

*State Key Laboratory of Heavy Oil Processing, China University of Petroleum, Beijing 102249,
China*

*Corresponding author.

E-mail address: daixp@cup.edu.cn

Synthesis of CoP/P-NiO/NF: Firstly, a certain amount of NaH₂PO₄ was dissolved in 15 mL H₂O₂ solution (30 vol. %), added 10 mL deionized water and transferred into a high-pressure reactor (50 mL) after stirring. A piece of clean nickel foam (NF) with a size of 2×3 cm was immersed into the above solution and kept 140 °C for 24 h to obtain the precursor of P-Ni(OH)₂/NF. Then, the solution of a certain amount of Co(NO₃)₂·6H₂O and 15 mL H₂O₂ solution (30 vol. %) was completely dissolved in 10 mL deionized water, and was transferred into a 50 mL high-pressure reactor containing Co(OH)₂/P-Ni(OH)₂/NF to hold 140 °C for 24 h. Finally, Co(OH)₂/P-Ni(OH)₂/NF was further phosphatized at 350 °C for 2 hours in a nitrogen atmosphere with 500 mg NaH₂PO₂ to obtain CoP/P-NiO/NF.

Calibration of reference electrode

The calibration of reference electrode was performed in the high purity hydrogen saturated electrolyte with two Pt foils as the working electrode and counter electrode, respectively. The Fig. S1 showed that the CV measurement was carried out at sweep rate of 1 mV s^{-1} in 1 M KOH electrolyte to determine the zero current potential, and the average (-0.9024) of the two potentials at which the current crossed zero was taken to be the thermodynamic potential, thus the relation between the Hg/HgO reference electrode and reversible hydrogen electrode (RHE) in 1 M KOH solution can be estimated by using formula: $E_{\text{RHE}} = E_{\text{Hg/HgO}} + 0.9024 \text{ V}$.

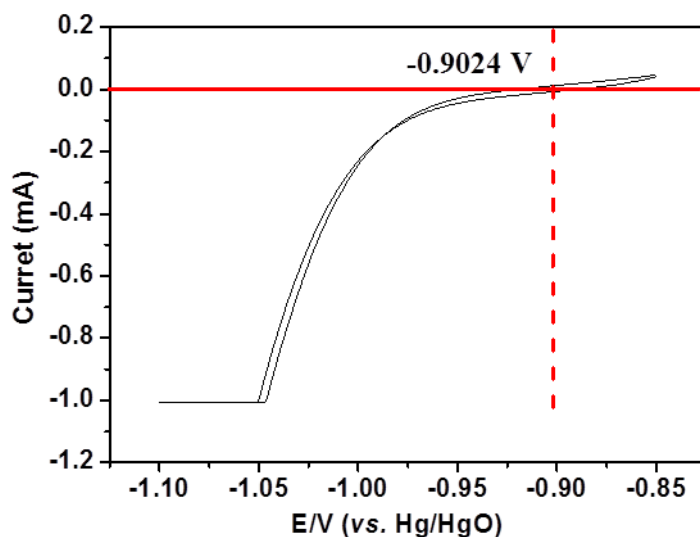


Fig. S1. The CV curves (1 mV s^{-1}) of the calibration of the HgO/Hg reference electrode in 1 M KOH solution.

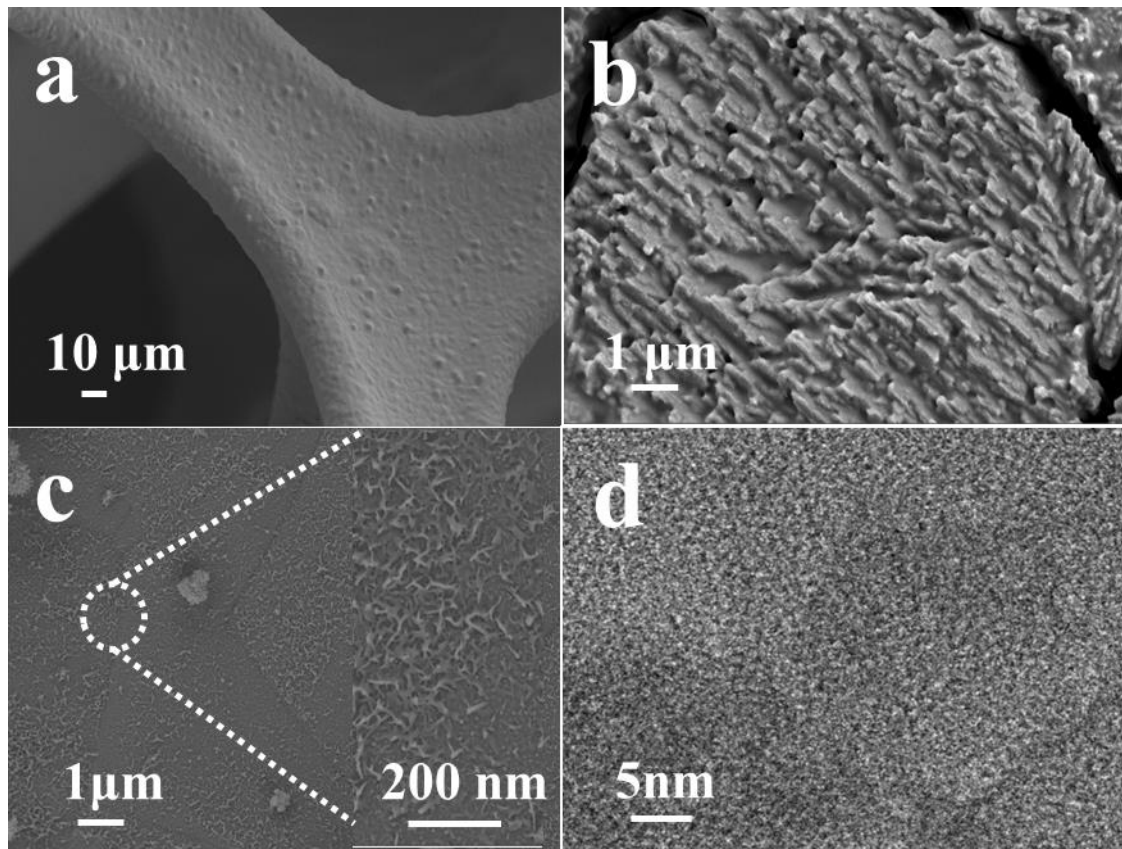


Fig. S2. SEM images of (a) NF, (b) pre-NF, (c) NiFe-HD/NF, (d) HRTEM image of Fe(OH)₃/pre-NF.

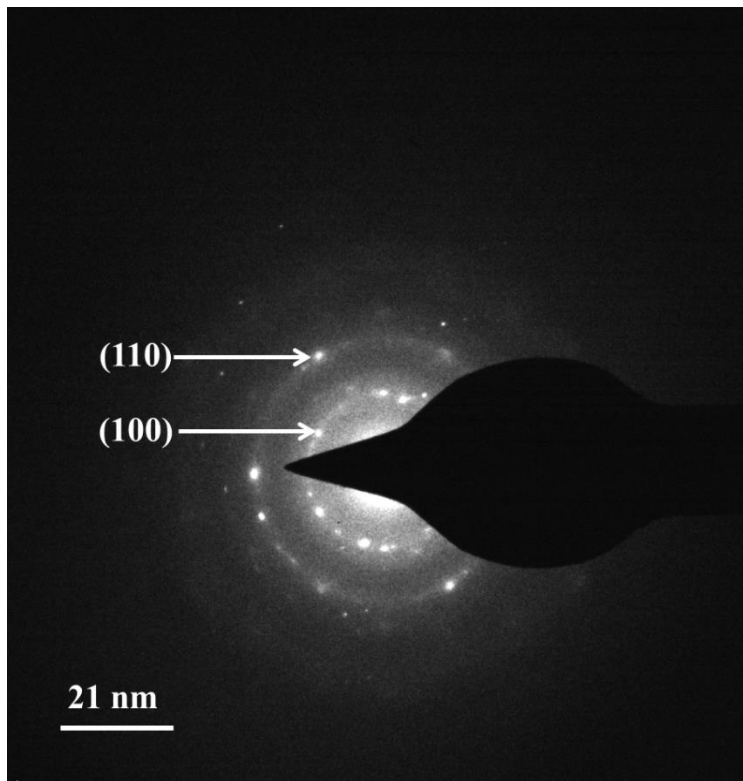


Fig. S3. SAED image of NiFe-HD peeling off from the NiFe-HD/pre-NF.

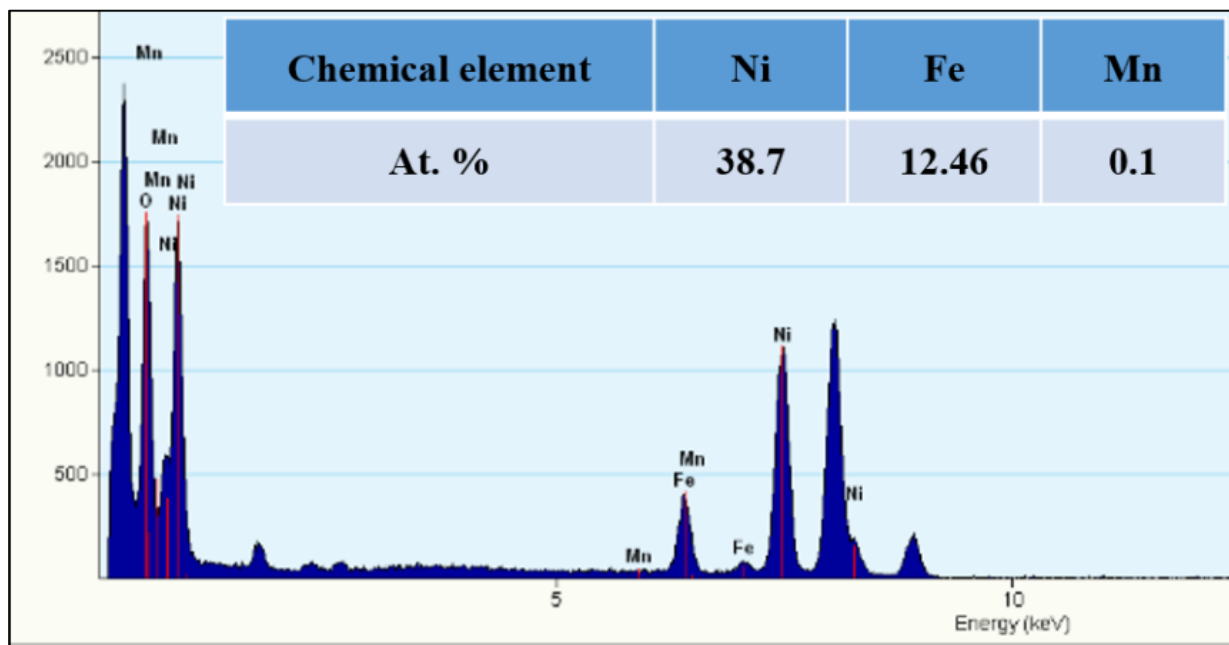


Fig. S4. TEM-EDS of NiFe-HD peeling off from the NiFe-HD/pre-NF.

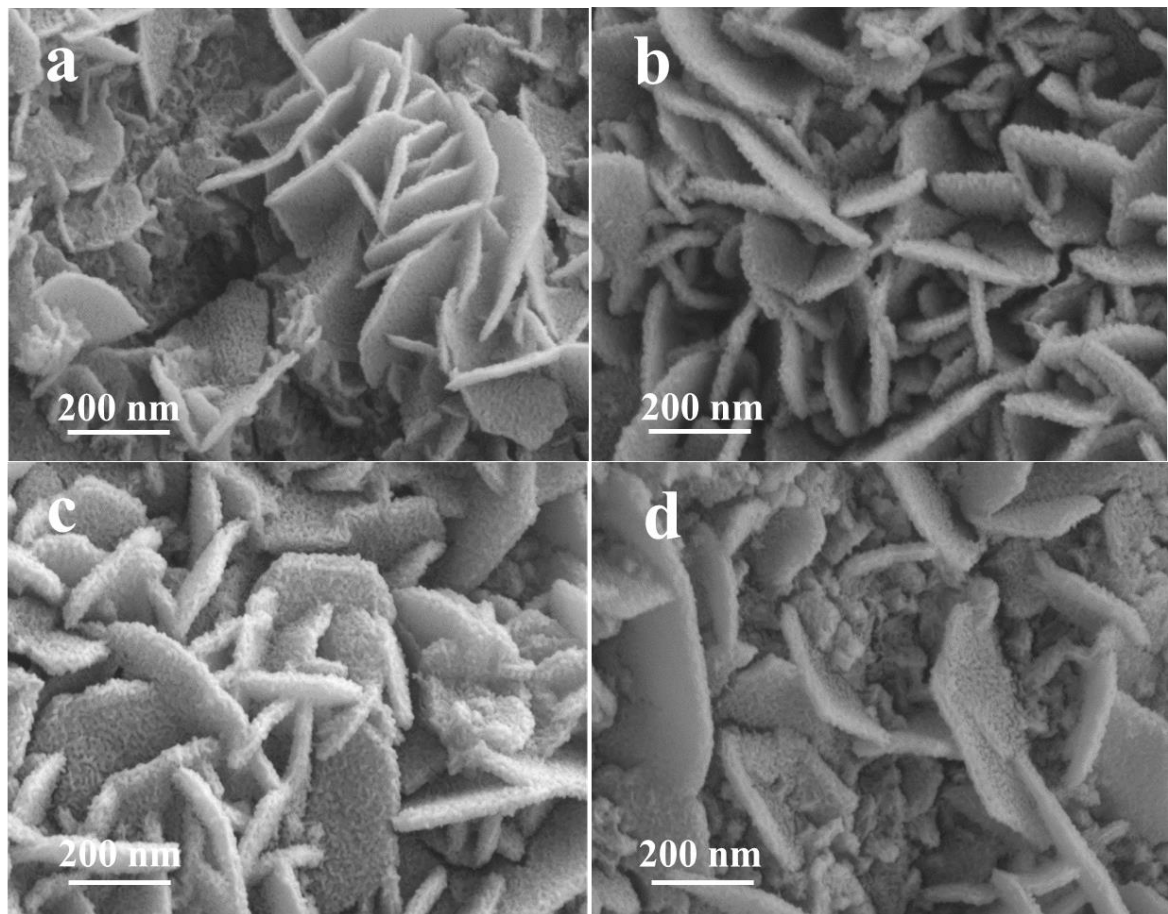


Fig. S5. SEM images of NiFe-HD/pre-NF with various electrodeposition time as (a) 20s, (b) 50s, (c) 100s and (d) 200s.

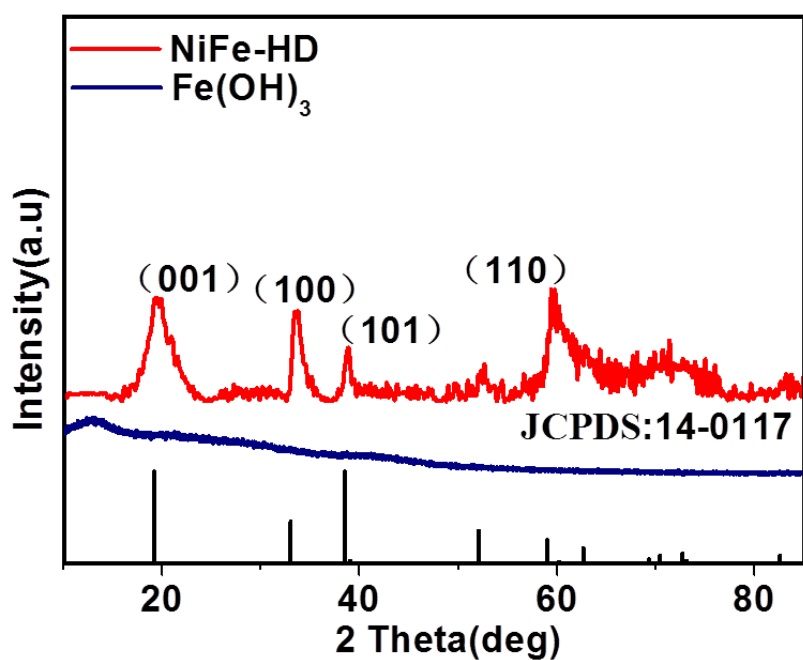


Fig. S6. XRD spectra of $\text{Fe}(\text{OH})_3$, NiFe-HD peeling off from the $\text{Fe}(\text{OH})_3/\text{pre-NF}$ and NiFe-HD/pre-NF, respectively.

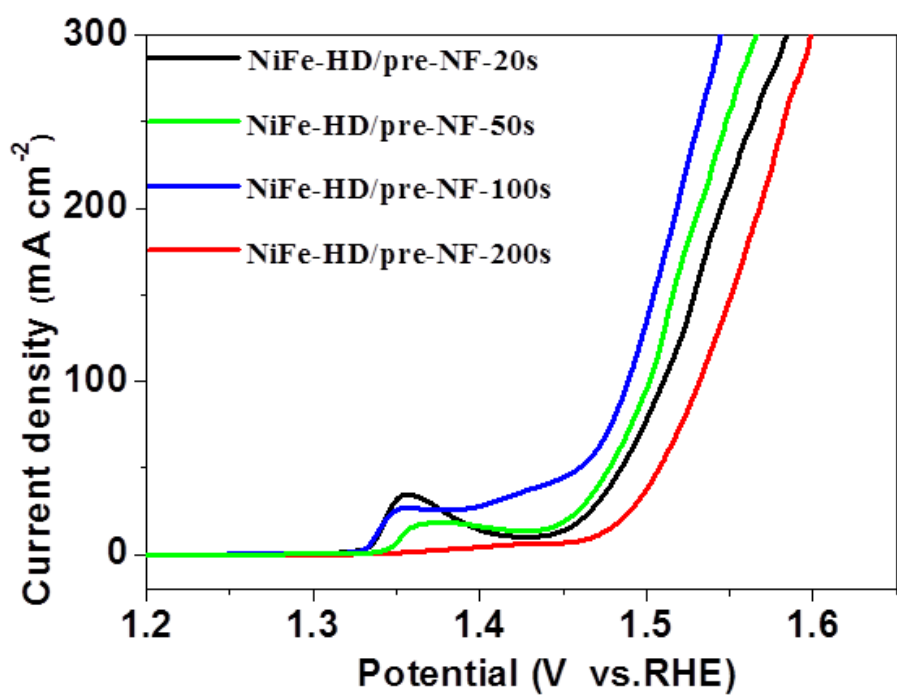


Fig. S7. Polarization curves after iR correction on the effect of electrodeposition time on NiFe-HD/pre-NF activity.

Table S1. Comparison of the OER performance of various catalysts in 1.0M KOH solution

Catalysts	η^{100} (mV)	Tafel (mV dec ⁻¹)	Ref.
NiFe-HD/pre-NF	256	81	This work
Fe(OH) ₃ /pre-NF	280	101	This work
β -Ni(OH) ₂ /pre-NF	390	117	This work
IrO ₂ /NF	360	-	This work
Fe-doped β -Ni(OH) ₂	280	53	[1]
Fe ₃ O ₄ /FeS ₂	306	48	[2]
Ni(OH) ₂ -NB	350	78.6	[3]
NiFe-LDH@NiCoP	220	48.6	[4]
NiCo ₂ O ₄ @NiMn-LDH	340	62.4	[5]
NiFe hydroxide film/GC	240	38.9	[6]
FeOOH NPs@ Ni-Fe LDH	270	37	[7]
amorphous CoFePi@crystalline Ni(PO ₃) ₂	320	39	[8]
NiCeO _x	390	85	[9]
NiFe(OH) _x /FeS/IF	265	-	[10]
α/β -Ni(OH) ₂ /CC	270	81	[11]
Co _x Fe _y N-NPs/graphene -sheets	292	32	[12]
CoNi-S/NS-rGO-550	470	79.5	[13]
NiFeSn@NiFe(O)OH	310	50	[14]

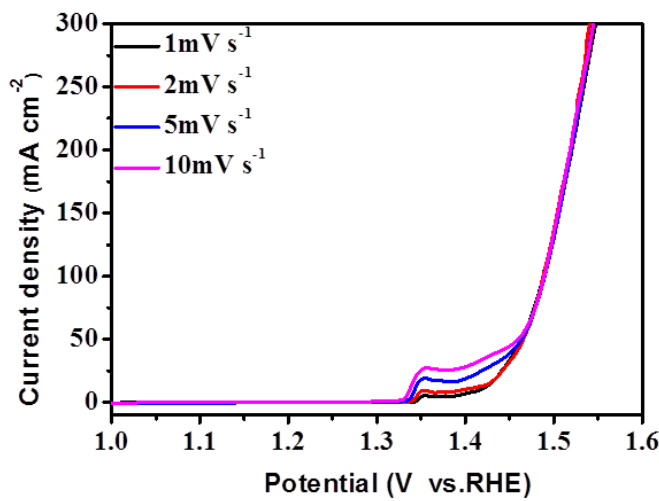


Fig. S8 LSV curves of NiFe-HD/pre-NF in 1.0 M KOH solution with different sweep slope.

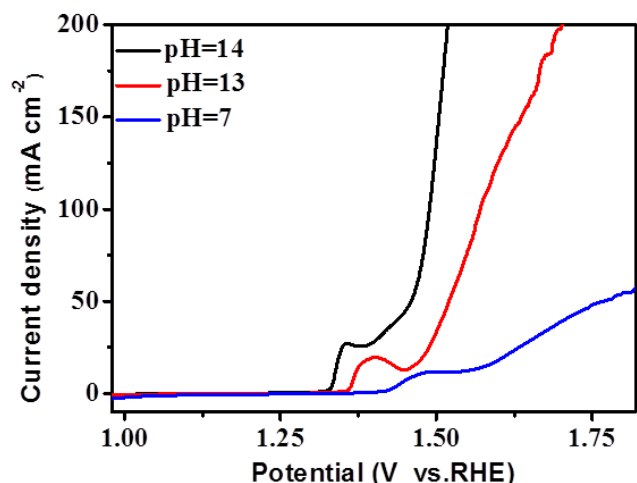


Fig. S9 LSV curves of NiFe-HD/pre-NF in KOH solution with different pH.

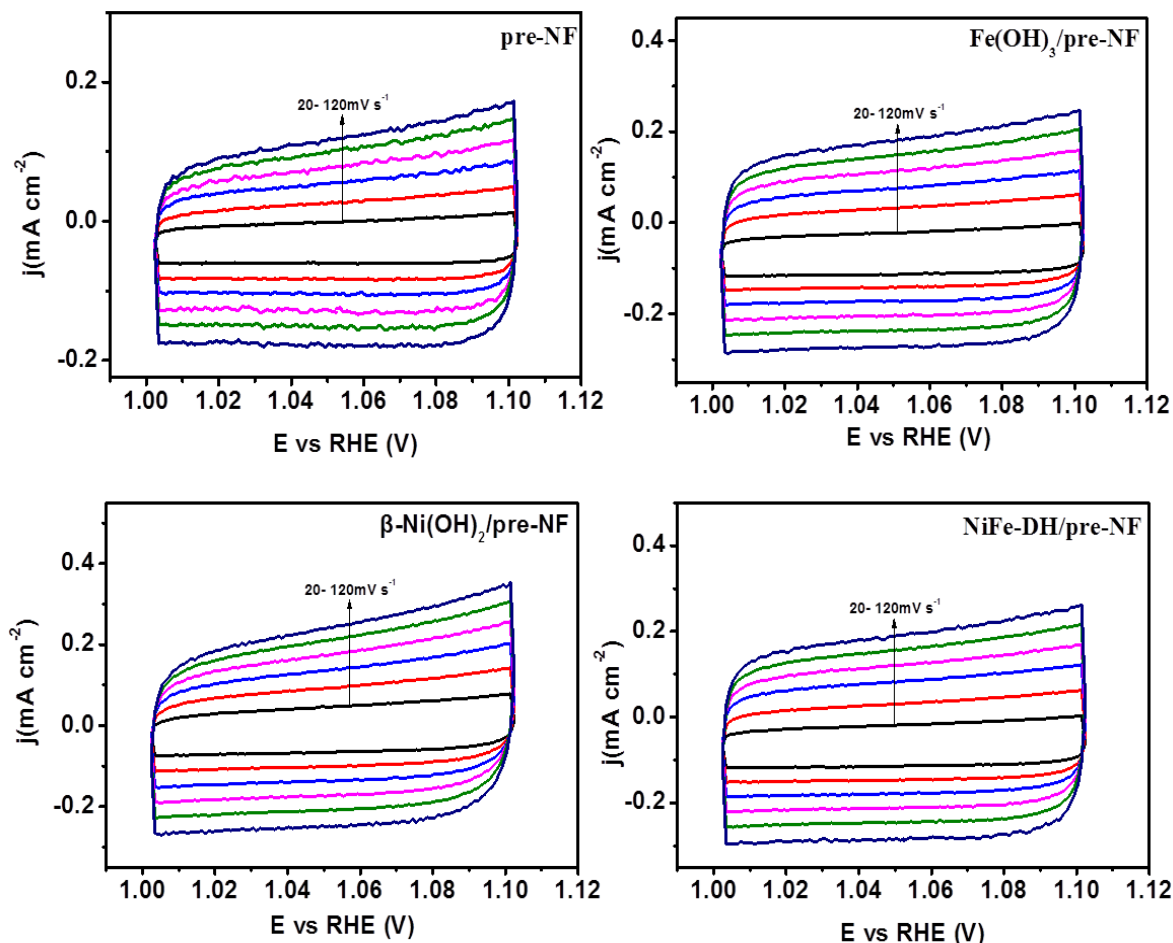


Fig. S10. (a-d) CV curves of pre-NF, $\text{Fe(OH)}_3/\text{pre-NF}$, $\beta\text{-Ni(OH)}_2/\text{pre-NF}$, NiFe-HD/pre-NF at scan rate of 20 to 120 mV in the potential range between 1.0024 and 1.0124 V(vs. RHE).

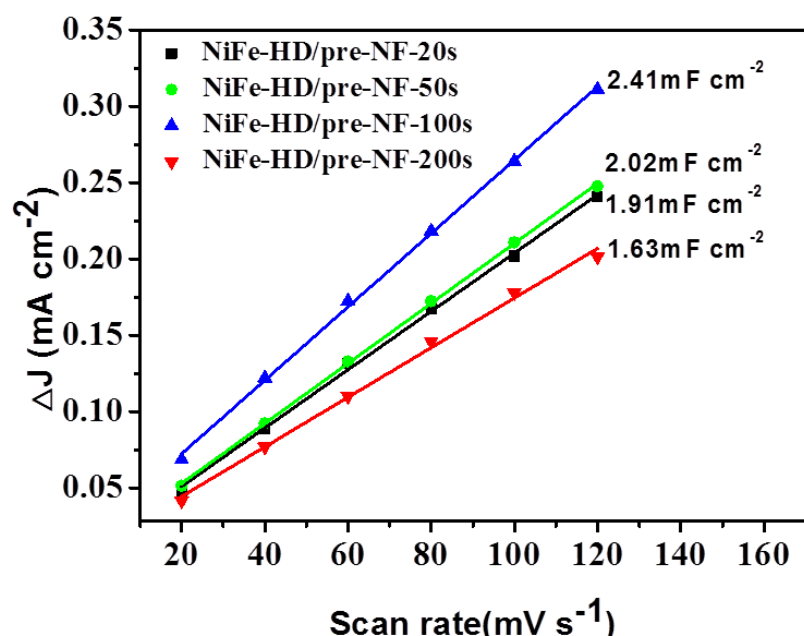


Fig. S11. Plots showing the extraction of the C_{dl} about the effect of electrodeposition time

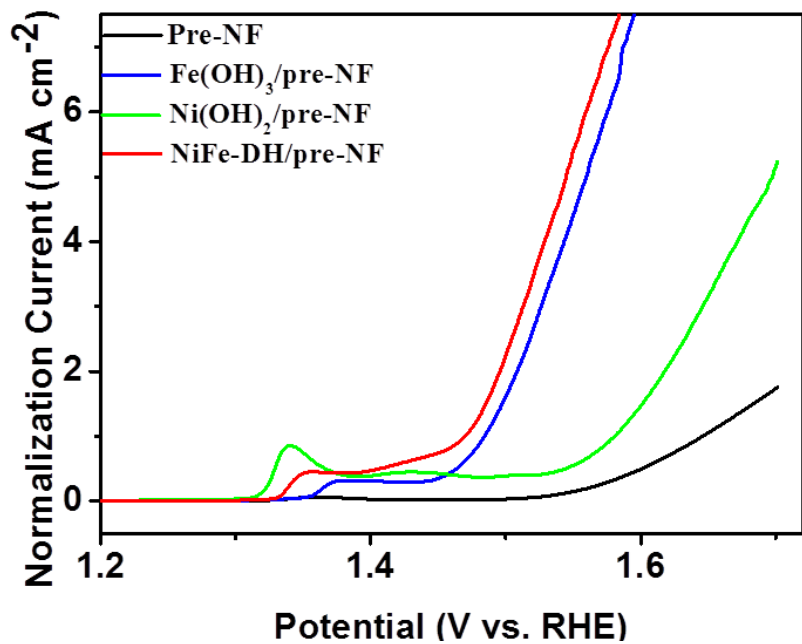


Fig. S12. Polarization curves based on ECSA.

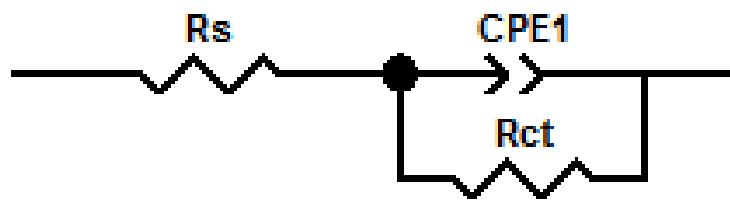


Fig. S13. The electrical equivalent circuit (EEC), Rs : the solution resistances, Rct : charge transfer resistances, $CPE1$: constant phase elements.

Table S2. The simulated equivalent circuit data of the catalysts

Sample	R _s [Ω]	CPE1-T	CPE1-P	R _{ct} [Ω]
Fe(OH) ₃ /pre-NF	0.80	0.06	0.87	0.60
Ni(OH) ₂ /pre-NF	0.83	0.06	0.86	7.0
NiFe-HD/pre-NF	0.82	0.10	0.90	0.38

Table S3. The ICP-MS data of the KOH solution

Electrolyte	Ni content (ppm)	Fe content (ppm)
pristine KOH	-	-
post- CV 3000 cyclic KOH	0.82	1.63

Table S4. Comparison of overall water splitting performance in recent reports and this work

Catalysts	Cell Voltages (V)			Stability (h)	Reference
	η_{10}	η_{100}	η_{300}		
NiFe-HD/pre-NF CoP/P-NiO/NF	-	1.62	1.77	85 h@100 mA cm⁻²	This work
IrO₂/NF Pt-C/NF	1.54	1.72	-	-	This work
NiFe(OH) _x /FeS/IF MoNi ₄ /MoO ₂ /NF	1.5	1.68	1.95	70 h@300 mA cm ⁻²	[10]
(Ni _x Fe _y Co _{6-x-y})Mo ₆ C/NF (Ni _x Fe _y Co _{6-x-y})Mo ₆ C/NF	1.47	1.60	1.70	50 h@500 mA cm ⁻²	[15]
Co@NC-600/NF Pt/C/NF	1.59	-	-	350 h@10 mA cm ⁻²	[16]
CF/VGSs/MoS ₂ /FeCoNi(OH) _x CF/VGSs/MoS ₂ /FeCoNi(OH) _x	1.37	1.59	1.70	10 h@500 mA cm ⁻²	[17]
NiFeP-CNT@NiCo/CP NiCoP-CNT@NiCo/CP	1.58	1.91	-	100 h@10 mA cm ⁻²	[18]
NiFe(OH) _x @Ni ₃ S ₂ /MoS ₂ -CC (Ni ₃ S ₂ /MoS ₂ -CC	1.55	1.71	1.90	48 h@20 mA cm ⁻²	[19]
NiFeCo LDH NiFeCo phosphide	1.47	1.58	1.65	70 h@50 mA cm ⁻²	[20]
Co ₅ Mo _{1.0} O NSs@NF Co ₅ Mo _{1.0} P NSs@NF	1.68	1.90	2.1	30 h@10 mA cm ⁻²	[21]
Ni@NCNTs/NF-L NiFe-L	1.52	2.1	-	10 h@100 mA cm ⁻²	[22]
C ₃ N ₄ -CNT-CF S-C ₃ N ₄ -CNT-CF	1.8	-	-	10 h@10 mA cm ⁻²	[23]
Ni _x Co _{3-x} O ₄ NiCo/NiCoO _x	1.75	-	-	10 h@15 mA cm ⁻²	[24]
Co _{1-x} Fe _x -LDH Ni _{1-x} Fe _x -LDH	1.59	1.88	-	24 h@25 mA cm ⁻²	[25]

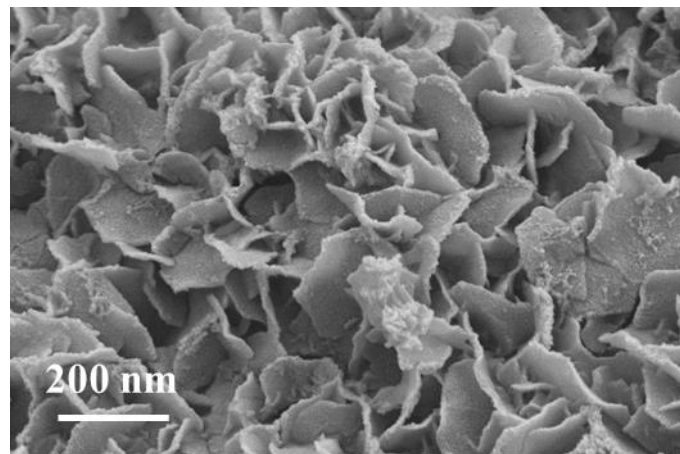


Fig. S14. SEM image of NiFe-HD /pre-NF after stability test

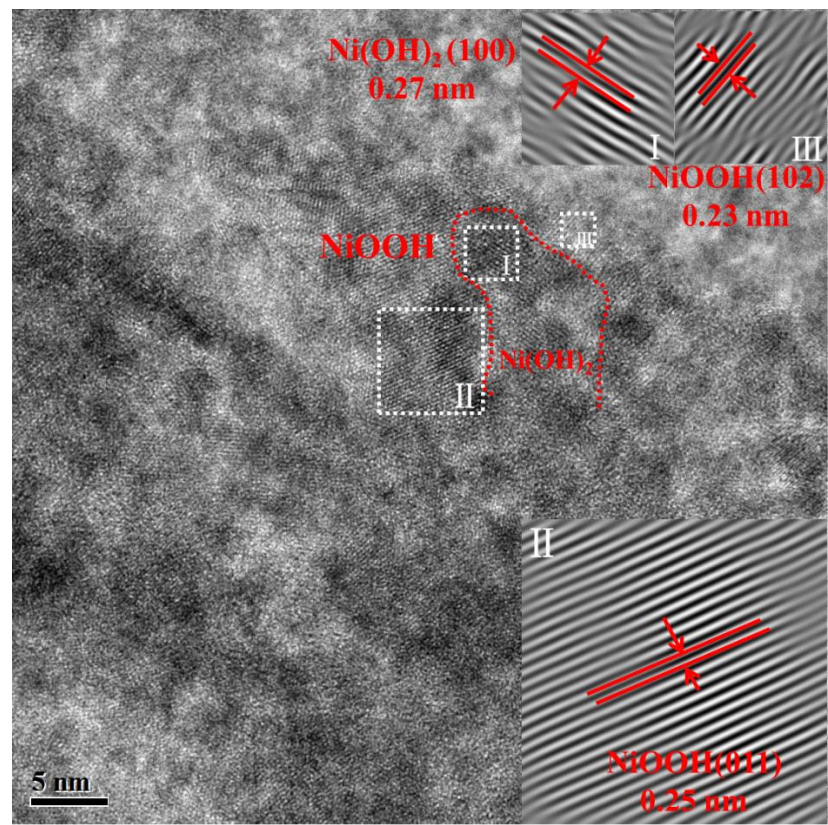


Fig. S15 HRTEM image of the NiFe-HD/pre-NF after 3000 CV cycles

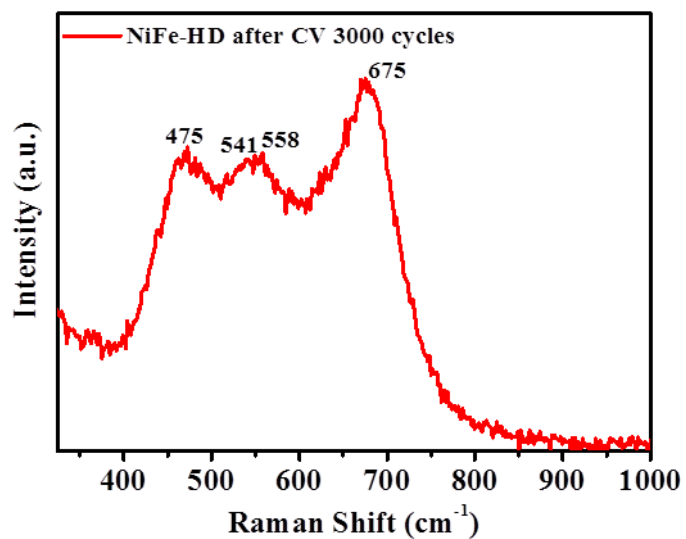


Fig. S16 Raman spectra of XPS spectra of NiFe-HD/pre-NF after 3000 CV cycles

Reference

- [1] T. Kou, S. Wang, J. L. Hauser, M. Chen, S. R. J. Oliver, Y. Ye, J. Guo and Y. Li, *ACS Energy Lett.*, 2019, **4**, 622-628.
- [2] M. J. Wang, X. Zheng, L. Song, X. Feng, Q. Liao, J. Li, L. Li and Z. Wei, *J. Mater. Chem. A*, 2020, **8**, 14145-14151.
- [3] C. Luan, G. Liu, Y. Liu, L. Yu, Y. Wang, Y. Xiao, H. Qiao, X. Dai and X. Zhang, *ACS Nano*, 2018, **12**, 3875-3885.
- [4] H. Zhang, X. Li, A. Hähnel, V. Naumann, C. Lin, S. Azimi, S. L. Schweizer, A. W. Maijenburg and R. B. Wehrspohn, *Adv. Funct. Mater.*, 2018, **28**, 1706847.
- [5] Z. Zhao, H. Wu, H. He, X. Xu and Y. Jin, *J. Mater. Chem. A*, 2015, **3**, 7179-7186.
- [6] W. Zhang, Y. Wu, J. Qi, M. Chen and R. Cao, *Adv. Energy Mater.*, 2017, **7**, 1602547.
- [7] J. Chen, F. Zheng, S.-J. Zhang, A. Fisher, Y. Zhou, Z. Wang, Y. Li, B.-B. Xu, J.-T. Li and S.-G. Sun, *ACS Catal.*, 2018, **8**, 11342-11351.
- [8] D.-C. Liu, L.-M. Cao, Z.-M. Luo, D.-C. Zhong, J.-B. Tan and T.-B. Lu, *J. Mater. Chem. A*, 2018, **6**, 24920-24927.
- [9] J. Yu, Q. Cao, Y. Li, X. Long, S. Yang, J. K. Clark, M. Nakabayashi, N. Shibata and J.-J. Delaunay, *ACS Catal.*, 2019, **9**, 1605-1611.
- [10] S. Niu, W. J. Jiang, T. Tang, L. P. Yuan, H. Luo and J. S. Hu, *Adv. Funct. Mater.*, 2019, **29**, 1902180.
- [11] P. Hao, W. Zhu, L. Li, Y. Xin, J. Xie, F. Lei, J. Tian and B. Tang, *Chem. Commun. (Camb)*, 2019, **55**, 10138-10141.
- [12] H. Liu, X. Lu, Y. Hu, R. Chen, P. Zhao, L. Wang, G. Zhu, L. Ma and Z. Jin, *J. Mater. Chem. A*, 2019, **7**, 12489-12497.
- [13] M. B. Zakaria, D. Zheng, U. P. Apfel, T. Nagata, E. S. Kenawy and J. Lin, *ACS Appl. Mater. Interfaces*, 2020, **12**, 40186-40193.
- [14] M. Chen, S. Lu, X. Z. Fu and J. L. Luo, *Adv. Sci. (Weinh)*, 2020, **7**, 1903777.

- [15] L.-G. He, P.-Y. Cheng, C.-C. Cheng, C.-L. Huang, C.-T. Hsieh and S.-Y. Lu, *Appl. Catal. B Environ.*, 2021, **290**, 120049.
- [16] A. Sivanantham, P. Ganesan, L. Estevez, B. P. McGrail, R. K. Motkuri and S. Shanmugam, *Adv. Energy Mater.*, 2018, **8**, 1702838.
- [17] X. Ji, Y. Lin, J. Zeng, Z. Ren, Z. Lin, Y. Mu, Y. Qiu and J. Yu, *Nat Commun*, 2021, **12**, 1380.
- [18] Z. Wang, C. Wei, X. Zhu, X. Wang, J. He and Y. Zhao, *J. Mater. Chem. A*, 2021, **9**, 1150-1158.
- [19] X. H. Wang, Y. Ling, B. L. Li, X. L. Li, G. Chen, B. X. Tao, L. J. Li, N. B. Li and H. Q. Luo, *J. Mater. Chem. A*, 2019, **7**, 2895-2900.
- [20] J. Lee, H. Jung, Y. S. Park, N. Kwon, S. Woo, N. C. S. Selvam, G. S. Han, H. S. Jung, P. J. Yoo, S. M. Choi, J. W. Han and B. Lim, *Appl. Catal. B Environ.*, 2021, **294**, 120246.
- [21] Y. Zhang, Q. Shao, S. Long and X. Huang, *Nano Energy*, 2018, **45**, 448-455.
- [22] H. Yuan, F. Liu, G. Xue, H. Liu, Y. Wang, Y. Zhao, X. Liu, X. Zhang, L. Zhao, Z. Liu, H. Liu and W. Zhou, *Appl. Catal. B Environ.*, 2021, **283**, 119647.
- [23] Z. Peng, S. Yang, D. Jia, P. Da, P. He, A. M. Al-Enizi, G. Ding, X. Xie and G. Zheng, *J. Mater. Chem. A* 2016, **4**, 12878-12883.
- [24] X. Yan, K. Li, L. Lyu, F. Song, J. He, D. Niu, L. Liu, X. Hu and X. Chen, *ACS Appl. Mater. Interfaces*, 2016, **8**, 3208-3214.
- [25] G. Rajeshkhanna, T. I. Singh, N. H. Kim and J. H. Lee, *ACS Appl. Mater. Interfaces*, 2018, **10**, 42453-42468.